Facile Synthesis and Structural Characterization of Chromium-doped Zinc Oxide Photocatalysts for Photo-removal of Methylene Blue under UV-light Intensity Irradiation

Suhailah Rosman[1], Hartini Ahmad Rafaie[2]*, Siti Nur Hidayah Yahya[1], Suraya Ahmad Kamil[1,3], Siti Nurbaya Supardan[1,3], Hamizah Mokhtar[4] and Zul Adlan Mohd Hir[4]

[1]Faculty of Applied Sciences, Universiti Teknologi MARA Selangor, 40450 Shah Alam, Selangor, Malaysia

[2]Centre of Foundation Studies, Universiti Teknologi MARA, Selangor Branch, Dengkil Campus, 43800 Dengkil, Selangor, Malaysia

[3]Centre for Nanomaterials Research, Institute of Science, Universiti Teknologi MARA Selangor, 40450 Shah Alam, Selangor, Malaysia

[4]Faculty of Applied Sciences, Universiti Teknologi MARA Pahang, 26400 Bandar Tun Abdul Razak, Jengka, Pahang, Malaysia

*Corresponding author (e-mail: hartinirafaie@uitm.edu.my)

Zinc oxide (ZnO) semiconductor-based photocatalysts are widely utilized in water treatment due to their high photocatalytic performance. Herein, pure ZnO and chromium (Cr)-doped ZnO with varying weight % (wt. %) of Cr (1, 3 and 5 wt.%) were synthesized using a chemical mixing method. The morphology, composition, and crystallinity of the synthesized samples were characterized by scanning electron microscopy (SEM), energy dispersive X-ray spectroscopy (EDX), and X-ray diffraction (XRD). Photocatalytic activity was assessed by monitoring the degradation of methylene blue (MB) dye under UV light exposure. SEM images reveal that Cr-doped ZnO particles exhibit a rod-cubic morphology with uniform distribution and good dispersion. EDX confirms the presence of Zn, O, and Cr without any impurities, verifying sample purity. XRD analysis indicates that Cr doping influences crystallinity, with an average crystallite size ranging from 35.20 nm to 35.70 nm. A slight peak shift observed with lower Cr doping level suggests substitutional incorporation of Cr^{3+} ions at Zn^{2+} sites, causing minor lattice distortions. Photocatalytic degradation experiments demonstrate that Cr doping enhances ZnO's performance. The 1 wt. % Cr-doped ZnO (CZ-1) photocatalyst demonstrates the highest activity, achieving 99.8% MB degradation with a rate constant, *k* of 0.0906 min^{-1}, surpassing both pure ZnO (CZ-0) and other Cr-doped variants (CZ-3 and CZ-5). The presence of Cr^{3+} ions enhance MB dye degradation by trapping electrons, reducing recombination, and generating reactive species under UV light. In conclusion, Cr-doped ZnO showed enhanced photocatalytic performance, making it a promising alternative for treating textile wastewater.

Keywords: Chromium; methylene blue; photocatalytic degradation; photocatalyst; zinc oxide

Received: October 2024; Accepted: January 2025

Water contains a range of pollutants, including heavy metals, anions, medications, personal care items, feed additives, and organic dyes. Organic dyes have become a prevalent water contaminant due to their emission from several sectors such as textile, paint, cosmetics, paper, and others, for example, methylene blue (MB), which is a widely used cationic dye known for its vibrant blue color and high water solubility. Organic dyes, because of their resistance to change, have harmful impacts on the aquatic ecology and may have negative effects on people when consumed in large quantities [1-2]. Dye effluents, when released into natural water bodies, are posing potential risks to the aquatic environment and human health [3]. Hence, the elimination of dyes from industrial wastewater is crucial to safeguard both human health and the aquatic environment. Various methods have been employed to treat textile effluents for dye removal, including physicochemical techniques (such as filtration, chemical coagulation, activated carbon adsorption, ultrafiltration, and ozonation), electrocoagulation (EC), chemical methods (such as reduction, oxidation, ion exchange, and neutralization), and biodegradation [4-5]. While some of these procedures may provide positive results, they come with a hefty price tag, as well as other drawbacks and restrictions [6]. Among these treatment methods, advanced oxidation processes (AOP), particularly photocatalysis, show promise as an alternative technique for the removal of dyes from wastewater. Photocatalysts can be used for dye removal in industrial settings through the process of photocatalytic degradation, which involves the use of semiconductor photocatalysts to absorb sunlight and degrade various environmental contaminants, including dyes [2]. Photocatalysts are cost-effective and can be synthesized using common materials. They

are also environmentally friendly, as they do not produce any harmful byproducts. Photocatalysis involves the use of light and catalysts to speed up chemical reactions, and it can be either homogeneous or heterogeneous, depending on the photocatalysts used. There is a rising interest in heterogeneous composites involving metal oxides or sulfides, owing to their distinctive electrical, structural, photocatalytic, adsorbent, thermal, mechanical, and ability to occur at room temperature. For instance, metal oxides or sulfides such as ZnO, TiO_2, SnO_2, CuO and CdS are used as semiconductor photocatalysts [7- 9].

Zinc oxide (ZnO) is a widely studied photocatalyst due to its excellent properties, such as having a wide band gap (3.37 eV), strong UV absorption, high electron mobility and chemical stability, making it highly effective for various environmental and energy applications, particularly in water treatment and air purification [10-11]. Its abundant availability, low cost, and non-toxic nature also make ZnO an attractive material for sustainable photocatalytic processes [12]. Additionally, ZnO's ability to form diverse nanostructures enhances its surface area, improving the efficiency of light absorption and the generation of electron-hole pairs which is crucial for photocatalytic reactions. However, ZnO as an individual photocatalyst has its limitations too, such as low absorption in the visible light spectrum and the rapid recombination of photo-generated charge carriers, which reduces its photocatalytic efficiency [13-14]. Addressing these limitations often involves doping with metals or coupling ZnO with other semiconductors to extend its activity into the visible spectrum and improve charge separation. It has been reported that doping ZnO with transition metals can enhance the ZnO photocatalytic degradation efficiency by reducing bandgap energy and delaying the recombination rate of photogenerated electron-hole pairs. This will increase the production of reactive species for the degradation of dye pollutants and improve photocatalytic activity [15]. To overcome these drawbacks, doping ZnO with transition metals has been extensively explored as a strategy to enhance its photocatalytic performance.

Among various transition metals, chromium (Cr) has gained much attention recently because its doping improves photocatalytic activity in UV light and even enables the activation of the photocatalyst in visible light [16-17]. Cr is an effective dopant that can significantly modify the electronic and structural properties of ZnO. Cr-doped ZnO offers several advantages: Cr narrows the band gap of ZnO, allowing for better utilization of visible light, thereby expanding ZnO's photocatalytic activity under sunlight. Additionally, the incorporation of Cr into the ZnO lattice improves charge separation by reducing the recombination rate of photo-generated electron-hole pairs, which enhances the overall photocatalytic efficiency [18]. The dopant also influences the surface morphology and crystallinity of ZnO, further improving its performance in catalytic applications. While Cr doping enhances the photocatalytic properties of ZnO, the potential toxicity of Cr, particularly in its hexavalent form (Cr^{6+}), must be fully considered. Hexavalent chromium is recognized as a carcinogen and presents significant environmental and health risks. For photocatalyst, Cr utilized as a dopant to ZnO is typically present in its trivalent form (Cr^{3+}), making it significantly less toxic and more stable. Furthermore, the controlled incorporation of Cr^{3+} into the ZnO lattice minimizes the risk of environmental contamination or health hazards, making it a viable candidate for photocatalytic applications. Incorporation of Cr^{3+} ions, with an ionic radius of 0.62 Å, can easily penetrate the ZnO lattice due to their comparable size to Zn^{2+} ions, which has an ionic radius of 0.72 Å [19-20]. This similarity in size allows Cr^{3+} to substitute Zn^{2+} in the ZnO crystal structure without causing significant lattice distortion. In photocatalysis, Cr^{3+} doping improves charge separation by reducing the recombination rate of electron-hole pairs, leading to more efficient photocatalytic reactions. Overall, Cr^{3+} doping significantly enhances the photocatalytic performance of ZnO, making it more effective for environmental remediation and other catalytic applications. For instance, Jincy Mathai et al. [19] reported an enhancement in the photocatalytic performance of Cr-doped ZnO nanoparticles for methylene blue dye under visible light irradiation due to the presence of defects in the lattice, eventually leading to the reduction of the electron-hole recombination rate. Mahesha et al. [21] studied and reported the photodegradation of chromium-doped ZnO nanoparticles in the visible wavelength region against malachite green dye, reaching the maximum of 95.4% degradation. This excellent photocatalytic degradation performance of Cr/ZnO was also influenced by Cr dopant concentration which affected the reduction in the crystallite size, thus might match the optimum energy band gap required for the photocatalytic activity. Furthermore, Alkallas et al. [18] evaluated the photocatalytic degradation of methyl orange (MO) under UV-vis light illumination under 100 min irradiation time, which suggests that the increment in photocatalytic activity of Cr-doped ZnO is due to a high-density defect in the nanorods' structure.

In the present study, a facile chemical mixing method was used to synthesize Cr-doped ZnO at different weight percentages. The obtained samples were characterized using scanning electron microscope (SEM) equipped with energy dispersive X-ray (EDX) and X-ray diffraction (XRD). The performance evaluation of the photocatalytic applications was studied for the degradation of MB dye under UV light exposure. Thus, this study aimed to provide insights into optimizing Cr doping levels for improved photocatalytic degradation efficiency of dyes in wastewater treatment applications.

Table 1. Designation of photocatalyst samples.

Sample	Weight of ZnO (g)	Weight of source of Cr (g)	wt.% of Cr/ZnO
CZ-0	4.00	0.00	0
CZ-1	3.88	0.12	1
CZ-3	3.80	0.20	3
CZ-5	3.72	0.28	5

EXPERIMENTAL

Chemicals and Materials

All reagents used were of analytical grade and utilized as received without purification. Zinc oxide (ZnO) powder (particle size: 1-100 nm, 99.9 %) was purchased from Sigma-Aldrich (Selangor, Malaysia). Chromium(III) nitrate nonahydrate ($Cr(NO_3)_3.9H_2O$, 99%), sodium hydroxide (NaOH, 95%), and methylene blue (MB, 95%) were also supplied by Sigma-Aldrich (Selangor, Malaysia). Deionized (DI) water and acetone (CH_3COCH_3, 99.5%) were used as well throughout the experimental procedure.

Preparation of Cr-doped ZnO Photocatalysts

The Cr-doped ZnO photocatalysts were synthesized by a facile chemical mixing method at different weight % (wt. %). Initially, 3.88 g of ZnO powder was mixed with 0.12 g of chromium(III) nitrate nonahydrate ($Cr(NO_3)_3.9H_2O$) and dispersed in 100 mL of deionized water with continuous stirring for 1 h. The next step involved the gradual addition of 2.0 M sodium hydroxide to the stock solution drop by drop until the pH reached 10, which was monitored using a pH meter. Simultaneously, the solution was heated on a magnetic stirrer at 100°C with a stirring speed of 400 revolutions per minute for 1 hour, leading to the formation of a white precipitate. The precipitate was then washed three times with deionized water to remove any residual impurities. Finally, the obtained white precipitate was annealed in a furnace at 400°C for 24 hours and identified as CZ-1. Other Cr-doped ZnO samples were prepared using the same process at different wt.% of Cr to ZnO (3 and 5 wt.%) and labeled as CZ-3 and CZ-5, respectively. Pure ZnO labeled as CZ-0 was also prepared without the addition of Cr for comparison purposes. Table 1 shows the composition of the prepared photocatalysts. The phase and crystalline characteristics of the prepared Cr-doped ZnO were characterized using X-ray diffraction (XRD) (PAN analytical with Cu-Kα radiation probe beam of 1.54056 Å wavelength) with 20-90° range. The morphology, elemental composition, and mapping of Cr-doped ZnO were determined by scanning electron microscope (SEM-EDX, TESCAN VEGA3), equipped with an energy dispersive X-ray analyzer.

Photocatalytic Performance Evaluation

Photocatalytic degradation was measured based on the decomposition of methylene blue (MB) dye as the test solution to assess the photocatalytic degradation efficiency of pure ZnO and Cr-doped ZnO photocatalysts in aqueous solution at room temperature under UV light irradiation. The reaction was carried out using 20 mg of the test photocatalyst dispersed and suspended in a beaker containing 100 ml of MB dye solution (5 mg/L) and irradiated by UV light as illustrated in Figure 1. The suspension was vertically irradiated by the UV lamp (UV source, λ = 254 nm, 8 W) under constant stirring. Before irradiation, the working solution was magnetically stirred in the absence of light for 30 minutes to create the MB solution's adsorption desorption equilibrium. The solution was then exposed to UV light for 60 minutes while being continuously stirred. At 10-minute intervals and up to 60 min, about 5 mL of the liquid sample was collected and filtered to remove the photocatalyst. The residual concentration of MB in the sample was monitored by measuring the absorbance at 664 nm using a UV-Vis spectrometer at room temperature and converting the data into the corresponding concentration (C). In this study, the photocatalytic percentage degradation of MB was calculated using the following Eq. (1) [4].

$$Photocatalytic\ degradation\ of\ MB\ (\%) = \frac{C_0 - C_t}{C_0} \times 100\ \% \quad (1)$$

Where, C_0 represents the starting concentration of the MB solution and C_t represents the concentration of the MB solution at irradiation time t. Furthermore, using first-order kinetic rate reaction and the following equation Eq. (2) [22], the photodegradation rate constant, *k* values for the MB dye degradation at varied amounts of ZnO catalyst were calculated.

$$ln\frac{C}{C_0} = -kt \quad (2)$$

k was calculated from the graph of $\ln(C/C_0)$ vs irradiation time, where C_0 and C denote the MB dye concentration at time, t= 0 and t=t, respectively.

RESULTS AND DISCUSSION

X-ray Diffraction Analysis

X-ray diffraction (XRD) was employed to examine the phase structure and crystallinity of the samples. Figure 2 shows the XRD patterns of pure ZnO (CZ-0) and Cr-doped ZnO samples (CZ-1, CZ-3 and CZ-5) over a 2θ range of 20º - 90º. The XRD spectrum of CZ-0, shown in Figure 2(a), reveals the wurtzite structure, with the diffraction peak positions and intensities that closely match the standard reference (JCPDS card No: 36-1451) for the ZnO crystalline phase [19]. Prominent diffraction peaks are observed at (100), (002), (101), (102), (110), (103), (112), and (201) planes, corresponding to 2θ values of 32.07◦, 34.46◦, 36.18◦, 57.16◦, 63.10◦, 67.49◦ and 69.75◦, respectively, confirming the hexagonal wurtzite structure of ZnO. The XRD patterns for CZ-1, CZ-3, and CZ-5 (Figures 1(b)-(d)) indicate that the crystalline phase of ZnO is maintained even after doping with Cr, demonstrating that the primary structure of ZnO remains stable upon Cr incorporation. This is consistent with previous studies indicating that ZnO can retain its crystalline phase with low concentrations of the dopant [18].

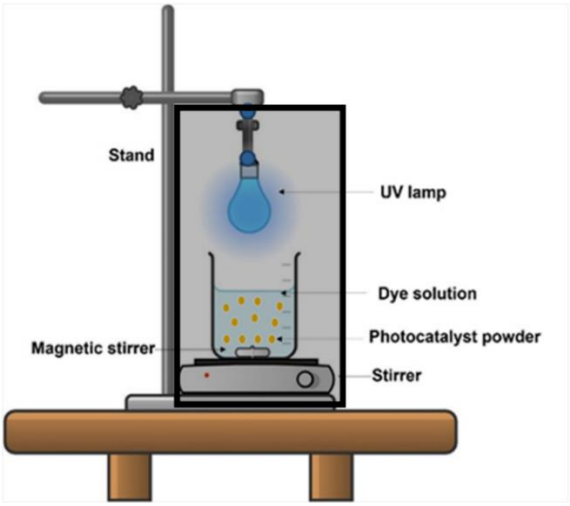

Figure 1. Schematic illustration of photoreactor setup for degradation of MB dye in aqueous solution using pure ZnO and Cr-doped ZnO photocatalysts with varying weight percentage of Cr (1, 3 and 5 wt.%). ($C_{initial}$=5 mg/L, 20 mg catalyst, light source: UV lamp (λ =254nm)).

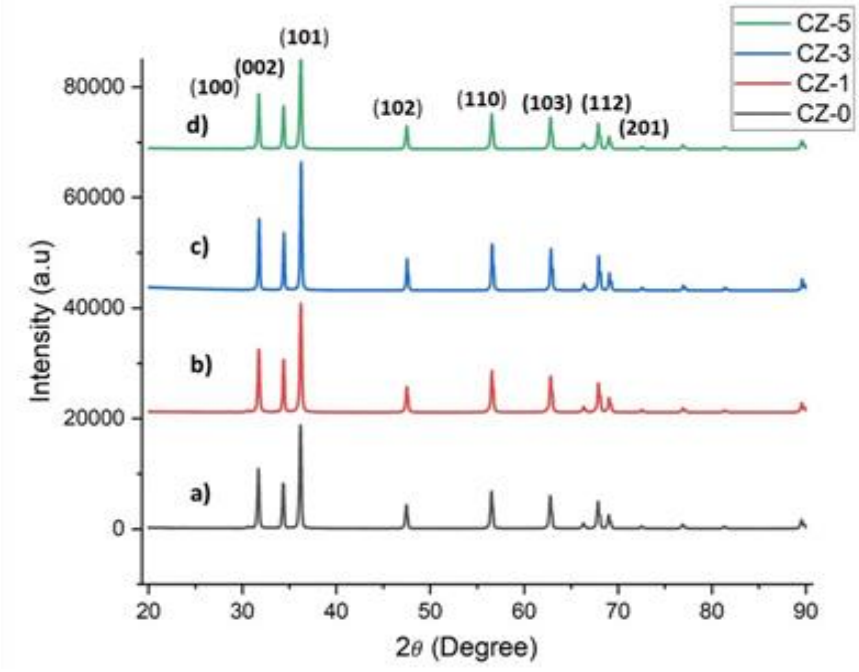

Figure 2. XRD patterns of (a) CZ-0, (b) CZ-1, (c) CZ-3, and (d) CZ-5.

As shown in Figure 2, the preferred crystal growth plane of ZnO is along the (101) direction and the average crystallite size was calculated using the Debye-Scherrer formula. The average crystallite size was estimated from the Debye–Scherrer's equation [23]:

$$D = \frac{k\lambda}{\beta \cos\theta} \quad (3)$$

Where, D is the crystallite size (nm), k is the Scherrer constant (typically 0.9), β is the full width at half maximum (FWHM) in radians, λ is wavelength of X-rays, and θ is the diffraction angle. The estimated crystallite size is found to be in the range 35.20–35.70 nm. The FWHM of major peaks decreases as Cr doping concentration increases, indicating a slight increase in the average crystallite size. This is in agreement with findings by Lokesha et al. (2023), who reported minimal peak shifts due to Cr^{3+} ions substituting Zn^{2+} sites in the lattice. Furthermore, the reduction in XRD peak intensity observed with higher Cr doping concentrations suggests an alteration in crystallinity. These changes are potentially linked to lattice strain induced by the substitution of Zn^{2+} with Cr^{3+} ions, which has a slightly different ionic radius [24]. This substitution leads to a minor lattice distortion within the ZnO wurtize structure due to Cr doping, which may alter the atomic scattering factor and result in peak broadening. Such lattice distortions can promote defects and charge trapping sites, enhancing charge separation and thus photocatalytic activity, as suggested by Shah et al. (2021) [25]. In this study, the absence of diffraction peaks from Cr dopant suggests that Cr is evenly distributed throughout the bulk phase of the Cr-doped ZnO. The absence of unidentified peaks further confirms the high purity and phase homogeneity of the synthesized Cr-doped ZnO samples.

Surface Morphological and Elemental Composition Analysis

The morphological analysis done for pure ZnO and Cr-doped ZnO at different weight percentages is presented in Figure 3. The SEM images at 5000x magnification illustrate the structures of (a) CZ-0, (b) CZ-1, (c) CZ-3, and (d) CZ-5, respectively. As depicted in Figures 3(a) – (d), the images reveal that both pure ZnO and the Cr-doped ZnO are composed of short, rod-cubic-like particles that are evenly distributed and well dispersed, with particle size ranging from 100 to 500 nm respectively. The formation and distribution of the Cr-doped ZnO samples (CZ-1, CZ-3, CZ-5) show notable changes compared to pure ZnO (CZ-0). It can be observed that the particles retain their original shape with only slight variations in surface structure, likely due to the incorporation of Cr during the synthesis. The SEM image for CZ-1 exhibits a slightly smaller particle and a uniform morphology, suggesting that the introduction of a low concentration of Cr has a minimal impact on the structural properties. As the Cr doping concentration increases (CZ-3 and CZ-5), the SEM images indicate a shift towards more irregular particle shapes and broader size distribution.

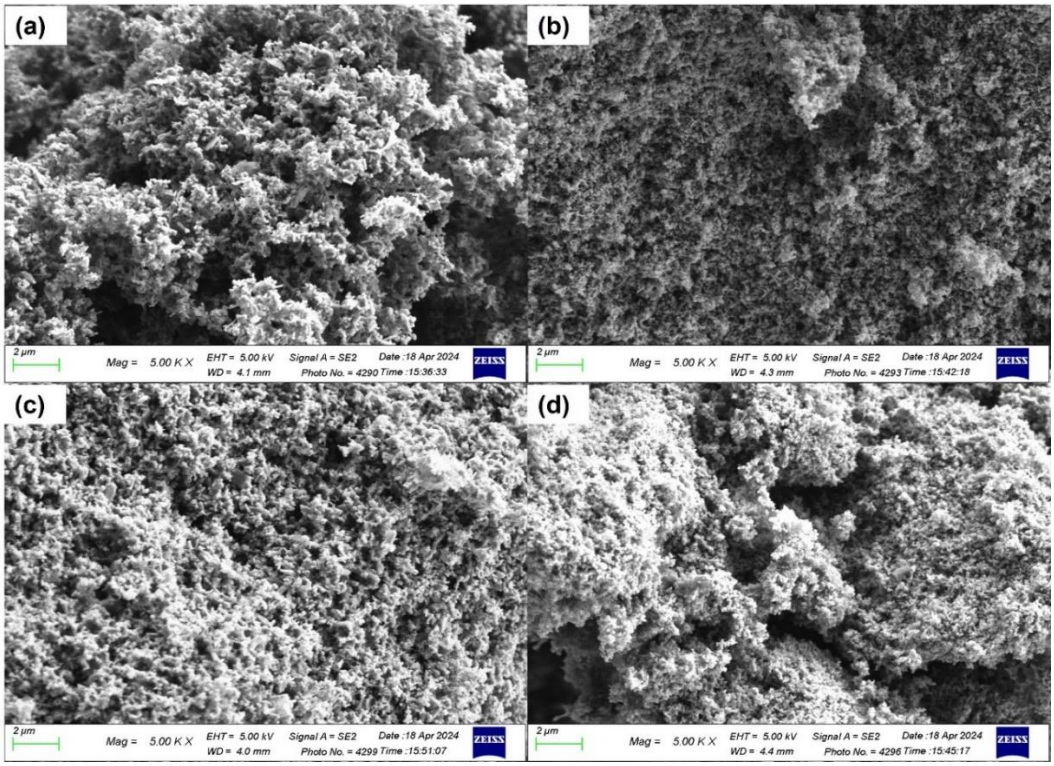

Figure 3. SEM images of (a) CZ-0, (b) CZ-1, (c) CZ-1, and (d) CZ-5 at 5000x magnification.

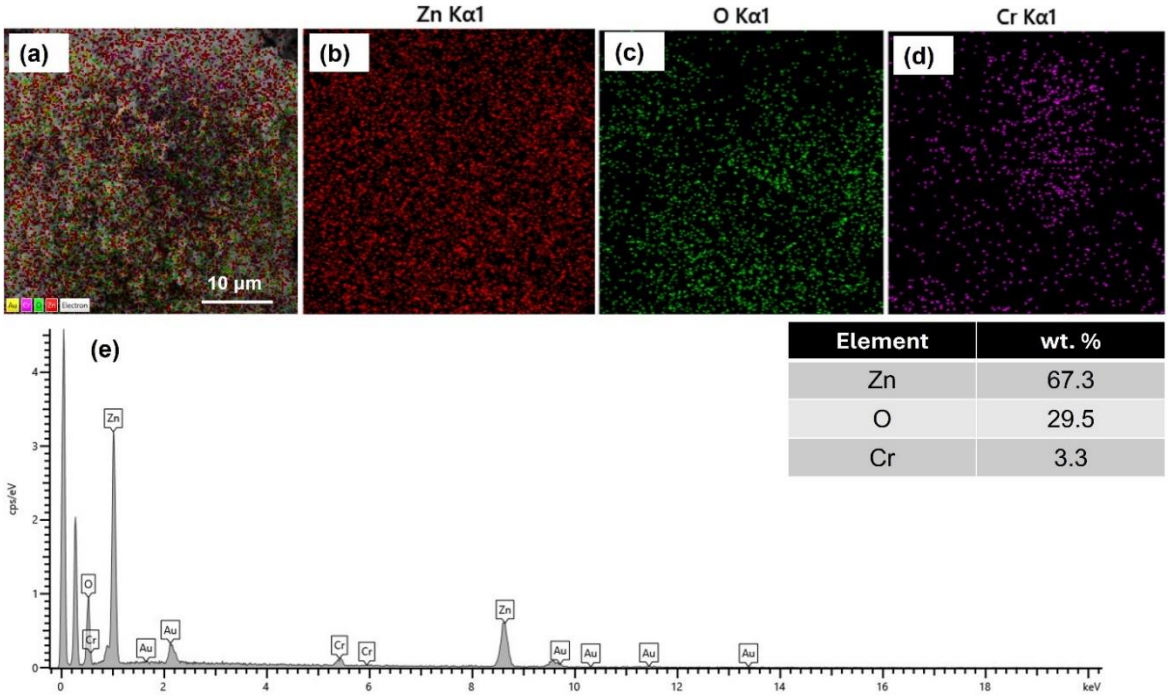

Figure 4. EDX analysis of selected CZ-1 photocatalyst with corresponding elemental mapping images for ZnO, O and Cr presented in (a), (b), (c) and (d), respectively, and (e) the elemental spectrum and composition of the sample.

Furthermore, rougher surface texture and more pronounced aggregation of particles becoming more apparent compared to CZ-1 could be attributed to the higher dopant levels. These changes could influence the photocatalytic properties by affecting the surface area and the number of active sites available for catalysis. On the other hand, a moderate increase in surface roughness can enhance photocatalytic performance by providing more active sites for photon absorption and reactive species generation. However, excessive particle aggregation can counteract these benefits by reducing the effective surface area and limiting the interaction between the photocatalyst and the target pollutant.

The EDX analysis was performed to complement the SEM findings and to further verify the presence of ZnO and Cr-doped ZnO samples. Figure 4 presents the EDX spectra and elemental mapping images for the selected sample CZ-1, showing the presence of Zn (Figure 4(a)), O (Figure 4(b)), and Cr (Figure 4(c)). The elemental spectrum (Figure 4(e)) shows no unexpected peaks, confirming that no extra elements are present in the samples. The EDX mapping images demonstrate a well-dispersed distribution of Cr within the ZnO matrix. Cr is effectively incorporated into the ZnO structure without forming separate clusters or phases, as evidenced by the uniform coloration across the mapping images. The presence of Cr, Zn, and O represented by red, green, and purple, respectively, suggests successful doping of Cr into ZnO. This finding aligns with the XRD results, which shows no secondary diffraction peaks that would indicate phase separation or impurities. These observations confirm that the Cr dopant is evenly embedded within the ZnO lattice, contributing to the overall homogeneity and stability of the material. The consistent integration of Cr is crucial for ensuring uniform photocatalytic performance across the sample surface, as an even distribution can lead to enhanced light absorption and efficient electron-hole pair generation during UV irradiation.

Photocatalytic Degradation Activity of Cr-doped ZnO Photocatalyst

Prior to the photocatalytic degradation process, the calibration curve of the MB in the aqueous phase was performed. The calibration curve was generated using the MB concentration of 5 to 25 mg/L. In this work, photocatalytic studies were performed using an initial MB concentration of 5 mg/L. After the photocatalytic degradation was completed, the absorbance of each sample was assessed to determine the residual concentration, as well as the percentage degradation (Figure 5). Figure 5(a) shows a gradual reduction in the maximum absorption peak of MB at 664 nm, indicating the decomposition of MB in the presence of the CZ-1 photocatalyst. This trend is similarly observed for other photocatalysts (CZ-0, CZ-3, and CZ-5), corroborating the visual observation of the MB solution turning colorless (Figure 5(d)).

The photocatalytic degradation efficiency for MB dye solution under UV irradiation was calculated using Equation (1), as outlined in methodology. Figure 5(b) presents the percentage degradation of MB dye as a function of irradiation time for all the samples under similar experimental conditions. The results demonstrate that no change is observed during the first 30 minutes before the light is turned on, as MB remains adsorbed on the catalyst's surface without undergoing decomposition under dark conditions. It is important to consider the potential effect of photolysis on the observed degradation. Photolysis refers to the direct decomposition of MB under UV-C light without the involvement of the photocatalyst. While a specific photolysis experiment was not conducted in this study, control experiments (Figure 5(b)) suggest that MB degradation in the absence of both UV light and the catalyst is negligible. Future work will include a dedicated photolysis study to isolate and quantify the effect of UV-C irradiation alone on MB degradation. Upon exposure to UV light, the degradation efficiency reaches approximately 95.2% for CZ-0, 99.8% for CZ-1, 83.8% for CZ-3, and 80.9% for CZ-5 after 60 minutes of irradiation. Among these, CZ-1 exhibits the highest photocatalytic performance, with 99.8% degradation. Although CZ-0 (pure ZnO) shows notable activity with 95.2% degradation, its lower efficiency compared to CZ-1 can be attributed to rapid recombination of photogenerated electron (e^-) - hole (h^+) pairs.

The higher photocatalytic activity of CZ-1 photocatalyst might be attributed to the role of chromium as an electron trap, which inhibits recombination of e^- and h^+ and enhances charge carrier separation, hence prolongs their lifetime [26]. In addition, this optimizes doping level, enhancing the photocatalytic activity by introducing defects that serve as active sites for photocatalytic reactions without significantly altering the surface area or morphology associated with minimal changes in morphology compared to pure ZnO. In contrast, the reduced performance of CZ-3 and CZ-5 (83.8% and 80.9%, respectively) suggests that excessive chromium ions doping leads to negative effects, such as increased aggregation and irregular morphology. These factors diminish the effective surface area and promote recombination, hence reducing the photocatalytic efficiency [27].

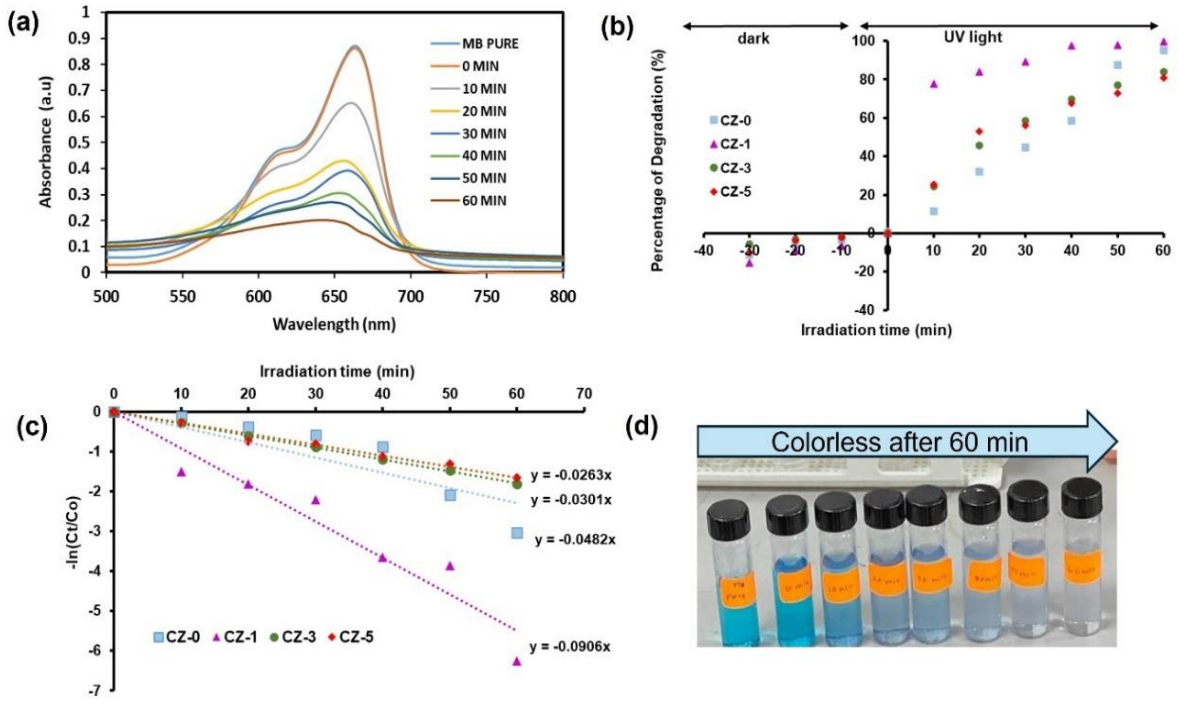

Figure 5. (a) UV-visible spectra of MB dye solution under UV lamp irradiation using CZ-1, (b) percentage degradation, (c) ln(C0/Ct) vs. reaction time (min), and (d) picture of MB dye solutions becoming colorless after 60 minutes ($C_{initial}$=5 mg/L, 20 mg catalyst, light source: UV lamp (λ =254nm)).

Table 2. Photocatalytic degradation activity of MB dye using pure ZnO and Cr-doped ZnO at different wt. % under UV lamp irradiation.

Photocatalyst	Degradation percentage (%)	Rate constant, k (min^{-1})	Correlation factor, R^2 Value
CZ-0	95.2%	0.0482	0.8550
CZ-1	99.8%	0.0906	0.9301
CZ-3	83.8%	0.0301	0.9993
CZ-5	80.9%	0.0263	0.9807

To have a better understanding of the reaction kinetics, the experimental data were fitted to a pseudo-first-kinetics model using Equation 2. Figure 5(c) depicts a plot of the linear kinetic fit of ln (C/Co) vs irradiation time for the photocatalytic degradation of MB dye by Cr-doped ZnO photocatalysts and the apparent rate constants, *k* are derived from the slope of the plots. According to the results, CZ-0 has an apparent reaction rate constant, *k* of 0.0482 min^{-1}, while CZ-1 has an apparent reaction rate constant, *k* of 0.0906 min^{-1}, correlating with its highest degradation percentage. In comparison, CZ-3 and CZ-5 have rate constants of 0.0301 and 0.0263 min^{-1}, respectively, further supporting the observation that excessive chromium doping reduces photocatalytic activity. The concentration of Cr plays a significant role. At low concentrations, Cr can create shallow traps that help in the separation of charge carriers, enhancing the photocatalytic activity [17]. However, at higher concentrations, excessive Cr can act as recombination centers, which might reduce the photocatalytic degradation efficiency. The performance of the photocatalyst based on the degradation percentage of MB, the photodegradation rate constant, *k* and the correlation factor, R^2 for the pure ZnO and Cr-doped ZnO at various wt.% are summarized in Table 2.

All samples exhibit an R^2 value between 0.8550 to 0.9993, suggesting a strong linear relationship and consistent degradation kinetics. In this experiment, the optimum amount of Cr dopant has resulted in a higher degradation percentage and degradation rate owing to an increase in the number of available surface-active sites on ZnO surfaces.

The proposed mechanism for the photocatalytic degradation of MB using Cr-doped ZnO is illustrated in Figure 6. When UV light carries photons with an equivalent or a greater energy than the photocatalyst incident on the photocatalyst, electrons in the valence band get excited and transferred into the conduction band (e_{CB}^-), leaving a hole (h_{VB}^+) on the ZnO [15, 28]. The incorporation of Cr induces defect states that trap electrons, thereby preventing recombination and allowing more charge carriers to participate in redox reactions. This process leads to the generation of reactive species of hydroxyl radicals (•OH) and superoxide anions (O_2^-), which are responsible for the degradation of MB pollutants. In addition, the photocatalytic activity results show that a suitable number of dopant ions can really boost photocatalytic activity; however, excessive dopant ions are detrimental [29]. Nevertheless, if the concentration of Cr is too high, the Cr-related energy levels can facilitate the recombination of electrons and holes, reducing the overall photocatalytic efficiency. Therefore, an optimal doping level is crucial for maintaining a balance between band gap reduction and charge carrier recombination.

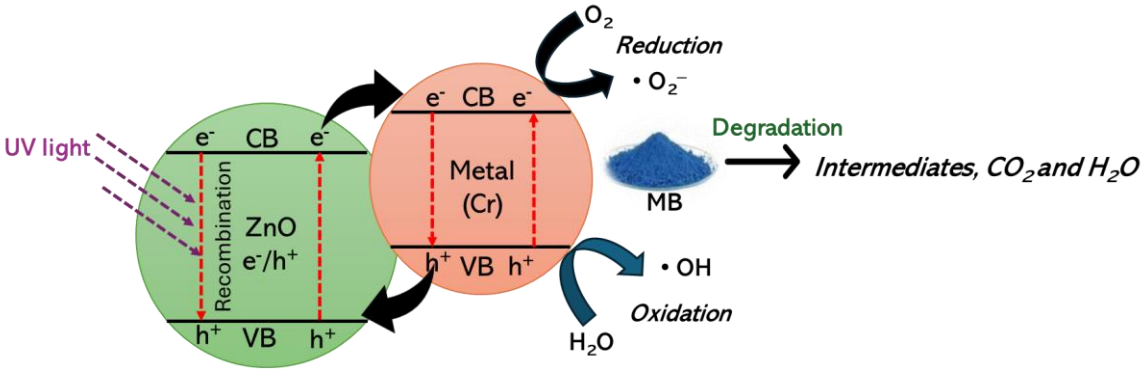

Figure 6. Illustration of MB degradation mechanism for Cr-doped ZnO photocatalyst

Table 3. A comparative study of Cr-oped ZnO photocatalysts in removal of dye pollutants from previous studies.

Photocatalyst	Method	Dye Pollutant	Source of light	Degradation percentage (%)	References
CZ-1 (the optimum)	Facile chemical mixing	MB	UV light	99.81	This study
Chromium-doped ZnO nanoparticles	sol–gel technique	MB	UV light	75.5	[16]
Cr-Doped ZnO Nanorods	thermal decomposition	methyl orange (MO)	UV light	99.8	[18]
Cr-doped ZnO nanoparticles	hydrothermal	MB	natural sunlight	52.2	[19]
1 mol% Cr 3+ doped ZnO	Auto-combustion	malachite green (MG)	Visible light	81.7	[21]
3 mol% Cr 3+ doped ZnO				83.7	
5 mol% Cr 3+ doped ZnO				84.4	
7 mol% Cr 3+ doped ZnO				89.4	
9 mol% Cr 3+ doped ZnO				95.4	

Table 3 provides a compilation of previous studies on investigating photocatalytic reactions using Cr-doped ZnO photocatalysts prepared by various methods for dye degradation. In the present study, the CZ-1 photocatalyst, prepared through a simple, cost-effective and scalable chemical mixing method, demonstrates superior photocatalytic performance under UV light. This method promotes uniform Cr distribution within the ZnO matrix, retains the sample purity, and produces a consistent cubic rod like structure across doping levels. Notably, the CZ-1 sample with 1 wt.% Cr achieved nearly complete degradation of MB, highlighting the advantages of optimized doping.

CONCLUSION

In summary, synthesizing Cr-doped ZnO photocatalysts at different weight percentages using a facile chemical mixing method, offers distinct advantages over conventional techniques, including simplicity, cost-effectiveness, and scalability. This approach enables uniform Cr distribution in the ZnO matrix, yielding pure samples with a consistent cubic-rod-like morphology, as confirmed by SEM and the EDX analysis which demonstrated the presence of Zn, O, and Cr without detecting any additional contaminants peak, demonstrating the purity of the samples. XRD results further revealed that the synthesized samples exhibited wurtzite crystal structure of ZnO. The addition of Cr enhanced the photocatalytic degradation efficiency of ZnO with an optimal doping level observed at 1 wt.% (CZ-1), achieving nearly complete degradation (99.8%) of MB within 1 hour under UV light, with a degradation rate constant, k of 0.0906 min^{-1} compared to other samples. Higher doping levels reduced photocatalytic efficiency, likely due to the formation of a recombination center that hindered electron-hole separation. These findings highlight the importance of optimizing doping levels to maximize the photocatalytic efficiency of ZnO.

ACKNOWLEDGEMENT

This research was funded by Ministry of Higher Education, Malaysia under the Fundamental Research Grant Scheme (Project No.: FRGS/1/2024/STG05/UITM/02/12), Kurita Water and Environment Foundation (KWEF) (Project No. 100-TNCPI/INT 16/6/2 (046/2024)) and Universiti Teknologi MARA (UiTM), Malaysia under the *Geran Penyelidikan Khas* (Project Number: 600-RMC/GPK 5/3 (190/2020). The authors would also like to acknowledge the services and facilities provided by UiTM Pahang Branch and UiTM Shah Alam to carry out the laboratory works.

REFERENCES

1. Momeni, A., Meshkatalsada, M. H., Bakhtiari, S. B. and Mousavi, Y. (2023) Photodegradation of methylene blue by phytosynthesized Ag–ZnO nanocomposites. *Hybrid Advances*, **3**, 100050.

2. Ahmad, I., Zou, Y., Jiaying, Y., Yuyu, L., Shazia, S., Yasin, N. M., Humaira, H., Qamar, K.W. and Khalid, N. R. (2022) Semiconductor photocatalysts: A critical review highlighting the various strategies

to boost the photocatalytic performances for diverse applications. *Advances in Colloid and Interface Science*, **311**, 102830.

3. Awais, M., Hussain, R., Shah, A., Alajmi, M. F., Maryam, R., Hussain, A., Khan, S. U. and Rahman, S. U. (2024) Design of novel FeSe2/ZnO composites and their application in photodegradation of methylene blue. *Physica B: Condensed Matter*, **685**, 416048.

4. Phuruangrat, A., Kuntalue, B., Thongtem, S. and Thongtem, T. (2021) Hydrothermal synthesis of hexagonal ZnO nanoplates used for photo-degradation of methylene blue. *Optik*, **226**, 165949.

5. Samarasinghe, L.V., Muthukumaran, S. and Baskaran, K. (2024) Recent advances in visible light-activated photocatalysts for degradation of dyes: A comprehensive review. *Chemosphere*, **349**, 140818.

6. Negash, A. , Tibebe, D., Mulugeta, M. and Kassa, Y. (2023) A study of basic and reactive dyes removal from synthetic and industrial wastewater by electrocoagulation process. *South African Journal of Chemical Engineering*, **46**, 122–131.

7. Kumar, J. V., Karthika, D., Rosaiah, P., Devanesan, S., Mythili, R., Dhananjaya, M. and Joo, S.W. (2024) Fabrication of SnO2/NGO hybrid nano-composite as an effective photocatalyst for binary dye degradation under sunlight illumination. *Process Safety and Environmental Protection*, **188**, 398–405.

8. Sultana, M., Mondal, A., Islam, S. and Afroza, M. (2023) Strategic development of metal doped TiO_2 photocatalysts for enhanced dye degradation activity under UV – Vis irradiation : A review. *Current Research in Green and Sustainable Chemistry*, **7**, 100383.

9. Uma, H. B., Kumar, M. S. V. and Ananda, S. (2022) Semiconductor-assisted photodegradation of textile dye, photo-voltaic and antibacterial property of electrochemically synthesized Sr-doped CuO nano photocatalysts. *Journal of Molecular Structure*, **1264**, 133110.

10. Abdullah, F. H., Bakar, N. H. H. A. and Bakar, M. A. (2022) Current advancements on the fabrication, modification, and industrial application of zinc oxide as photocatalyst in the removal of organic and inorganic contaminants in aquatic systems. *Journal of Hazardous Materials*, **424**, 127416.

11. Nawaz, A., Farhan, A., Maqbool, F., Ahmad, H., Qayyum, W., Ghazy, E., Rahdar, A., Díez-Pascual, A. M. and Fathi-karkan, S. (2024) Zinc oxide nanoparticles: Pathways to micropollutant adsorption, dye removal, and antibacterial actions - A study of mechanisms, challenges, and future prospects. *Journal of Molecular Structure*, **1312**, 138545.

12. Sazman, N. S. N., Rafaie, H. A., Daud, S., Mohd Shohaimi, N. A., Abu Bakar, M. A. A. and Hir, Z. A. M. (2023) Extraction and Physicochemical Characterization of Microcrystalline Cellulose from Gigantochloa scortechinii. *Malaysian Journal of Chemistry*, **25**, 323–330.

13. Widiyandari, H., Pratama, E. D., Parasdila, H., Suryana, R., Arutanti, O. and Astuti, Y. (2023) Synthesis of ZnO-Cdots nanoflower by hydro-thermal method for antibacterial agent and dye photodegradation catalyst. *Results in Materials*, **25**, 100491.

14. Izhar, N. I., Hir, Z. A. M., Rafaie, H. A. and Daud, S. (2024) Physicochemical Characterization of ZnO/G-C3 N4 For Photo-Removal of Methyl Orange Under Low UV-Light Intensity. *Malaysian Journal Analytical Science*, **28**, 365–375.

15. Bhapkar, A. R. and Bhame, S. (2024) A review on ZnO and its modifications for photocatalytic degradation of prominent textile effluents: Synthesis, mechanisms, and future directions. *Journal Environmental Chemical Engineering*, **12**, 112553.

16. Ray, R., Kumar, A., Paul, A. K. and Tyagi, S. (2016) Enhanced Photocatalytic Performance of Chromium Doped Zinc Oxide Nanoparticles. *Transactions of the Indian Institute of Metals*, **69**, 1043–1048.

17. Pavithra, M. and Jessie, R. M. B. (2024) Reusable porous chromium- zinc oxide nano-sheets for efficient detoxification of xenobiotics through integrated advanced oxidation water clean-up process. *Journal of Hazardous Materials Advances*, **13,** 100403.

18. Alkallas, F. H., Trabelsi, A. B. G., Nasser, R., Fernandez, S., Song, J. M. and Elhouichet, H. (2022) Promising Cr-Doped ZnO Nanorods for Photocatalytic Degradation Facing Pollution. *Applied Sciences*, **12**, 34.

19. Mathai, J., Anjana, M. P., Aleena, P. A., Thomas, S. A., Jose, K. A., Kunjumon, J., Nair, S. S., Rimal, R. S. I. and Sajan, D. (2023) Cr doped ZnO nanoparticles as photocatalyst for the degradation of methylene blue dye. *Journal of the Indian Chemical Society*, **100**, 9.

20. Jangannanavar, V. D., Basavanagoudra, H., Patil, M. K., Shettar, J. H., Inamdar, S. R. and Gourdae, K. M. (2024) Nanocrystal engineering: Unraveling bioactivities and augmented photocatalytic degradation of ZnO and Cr-doped ZnO via green and chemical synthesis routes. *Journal of Molecular Structure*, **1301**, 137340.

21. Mahesha, A., Nagaraja. M., Madhu, A., Suriyamurthy, N., Satyanarayana, S. R., Al-Dossari, Abd EL-Gawaad, M. N., Manjunatha, S. O., Gurushantha, K. and Srinatha, N. (2023) Chromium-doped ZnO nanoparticles synthesized via auto-combustion: Evaluation of concentration-dependent structural, band gap-narrowing effect, luminescence properties and photocatalytic activity. *Ceramic International*, **49**, 22890–22901.

22. Zhao, Y., Li, L., Zuo, Y., He, G., Chen, Q., Meng, Q. and Chen, H. (2022) Reduced graphene oxide supported ZnO/CdS heterojunction enhances photocatalytic removal efficiency of hexavalent chromium from aqueous solution. *Chemosphere*, **286,** 131738.

23. Patil, S. S., Chellachamy, A. A., Sukhdev, A. and Chandrasekaran, S. (2024) Facile one-pot synthesis of ternary Fe doped Cu-ZnO nanocatalyst: An efficient and recyclable solar light driven photocatalyst. *Surfaces and Interfaces*, **48**, 104255.

24. Lokesha, H. S., Prinsloo, A. R. E., Mohanty, P. and Sheppard, C. J. (2023) Impact of Cr doping on the structure, optical and magnetic properties of nanocrystalline ZnO particles. *Journal of Alloys and Compound*, **960**, 170815.

25. Shah, N. I., Jabeen, N., Irum, S., Ahmad, K. S., Tauseef, I., Khan, T. F., Anwaar, S., Shafique, S., Haleem, S. K., Mehmood, A. and Hussain, S. Z. (2021) Environmentally benign and economical bio-fabrication of ZnO and Cr-doped ZnO nanoparticles using leaf extract of Citrus reticulata for biological activities. *Materials Today Communications*, **27**, 102383.

26. Acedo-Mendoza, A. G., Infantes-Molina, A., Vargas-Hernández, D., Chávez-Sánchez, C. A., Rodríguez-Castellón, E. and Tánori-Córdova, J. C. (2020) Photodegradation of methylene blue and methyl orange with CuO supported on ZnO photocatalysts: The effect of copper loading and reaction temperature. *Material Science in Semiconductor Process*, **119**.

27. Mgidlana, S. and Nyokong (2021) A symmetrical zinc(II) phthalocyanines cobalt tungstate nano-material conjugates for photodegradation of methylene blue. *Journal of Photochemistry and Photobiology A: Chemistry*, **418**.

28. Li, X., Chen, Y., Tao, Y. 1, Shen, L., Xu, Z, Bian, Z. and Li, H. (2022) Challenges of photocatalysis and their coping strategies. *Chem. Catalysis*, **2,** 6, 1315–1345.

29. Saleh, R. and Djaja, N. F. (2014) Transition-metal-doped ZnO nanoparticles: Synthesis, characterization and photocatalytic activity under UV light. *Spectrochimica Acta - Part A: Molecular and Biomolecular Spectroscopy*, **130**.